Inorganic Chemistry

Article

pubs.acs.org/IC

# Inorganic and Organozinc Fluorocarboxylates: Synthesis, Structure and Materials Chemistry

A. L. Johnson,[†] A. J. Kingsley,[‡] G. Kociok-Köhn,[†] K. C. Molloy,*[,†] and A. L. Sudlow[†]

[†]Department of Chemistry, University of Bath, Claverton Down, Bath BA2 7AY, U.K.

[‡]SAFC Hitech, Power Road, Bromborough, Wirral CH62 3QF, U.K.

Supporting Information

**ABSTRACT:** The organozinc fluorocarboxylates $RZnO_2CR_f$ and $RZnO_2CR_f$·TMEDA, along with $Zn(O_2CR_f)_2$·TMEDA (R = Me, Et; $R_f$ = $C_2F_5$, $C_3F_7$) have been synthesized. The structures of $EtZnO_2C_2F_5$ (**5**), $EtZnO_2C_3F_7$ (**7**), $EtZnO_2C_2F_5$·TMEDA (**11**), $Zn(O_2C_2F_5)_2$·TMEDA (**13**), along with products from the adventitious reaction with either $O_2$ or $H_2O$, $Zn_{10}Me_4(OMe)_4(O_2CC_2F_5)_{12}$ (**2**), $Zn_9Et_2(O_2CC_2F_5)_{12}(O)_2$ (**6**), $Zn_8Et_4(OEt)_4(O_2CC_3F_7)_6(O)$ (**8**), $[Zn(O_2CC_3F_7)_2$·TMEDA$]_2$·$H_2O$ (**15**) have been determined. Thin films of oriented ZnO have been deposited on glass substrates by low-pressure chemical vapor deposition (LPCVD) using **3** and **10** as precursors, though no fluorine incorporation in the films was noted. LPCVD using **13** as precursor also yielded fluorine-free ZnO, but lacking the oriented growth observed using **3**, **10**. However, **5**, which exhibits short intermolecular Zn···F contacts in the solid state, thermally decomposes to bulk $ZnF_2$.

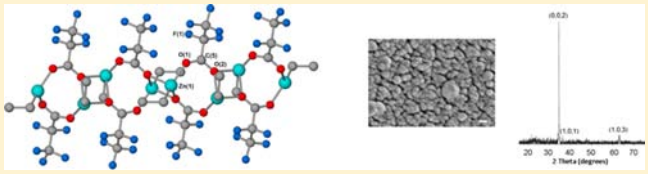

## INTRODUCTION

Zinc carboxylates have long attracted the interest of chemists because of their fundamental roles in biological systems,[1] as catalysts (for example, copolymerization of $CO_2$/epoxides,[2,3] cyclopropanation[4] among others[5]), hydrogen storage[6] and as secondary building units for a vast array of metal−organic frameworks (MOFs).[7−9] As a result, in excess of 5000 zinc carboxylate structures can be found in the Cambridge Crystallographic database, though, remarkably, only 16 are organozinc carboxylates of which 12 adopt a conventional $RZn(O_2CR')$ arrangement.

Our interest in this area is the possible use of volatile zinc carboxylates as precursors for ZnO materials. ZnO has a hexagonal wurtzite structure and is a wide bandgap semiconductor with a bandgap of 3.3 eV;[10] conductivity can be increased with the addition of dopants such as B,[11] Al,[12] Ga,[13] and In.[14] In particular, we are interested in fluorine-doped zinc oxide (ZnO:F)[15] as an alternative transparent conducting oxide (TCO) to the more common $In_2O_3$:Sn (ITO) or fluorine-doped tin oxide (FTO). In ZnO:F, fluorine atoms enter the ZnO lattice in substitutional form; Gordon et al. have theorized that because of this, fluorine doping gives the lowest resistivity to ZnO.[15] ZnO:F has been identified as having the highest transparency and being one of the least toxic TCOs, as well as being cheap and abundant, both prerequisites for sustainable commercial exploitation.[16]

Thin films of ZnO:F have been deposited using spray pyrolysis,[17] sol−gel spin coating,[18] and sputtering.[19] Gordon et al. have studied the deposition of ZnO:F by CVD extensively and have deposited films initially using a multisource approach, that is, $Et_2Zn$, EtOH, and $C_3F_6$ and later using $Et_2Zn$·TMEDA, EtOH, and $C_6H_5C(O)F$. The earlier precursors in particular grew high quality films with a very low sheet resistance of 5Ω/square and a visible absorption of 3%.[10,15] We have previously used organotin fluorocarboxylates to successfully deposit FTO,[20] and have now attempted to use the same methodology for ZnO:F. While a search of the Cambridge Crystallographic database reveals numerous structures containing the $Zn(O_2CCF_3)$ moiety, only two reports concern more fluorinated carboxylic acid derivatives of zinc.[21,22]

## EXPERIMENTAL SECTION

All operations were carried out under an atmosphere of dry dinitrogen or argon using standard Schlenk and glovebox techniques. Hexane, dichloromethane, and tetrahydrofuran solvents were dried using an Innovative Technology, Inc. Solvent Purification System (SPS) system and degassed under dinitrogen or argon prior to use. Deuterated tetrahydrofuran (THF) and chloroform ($C_6D_6$) NMR solvents were purchased from Aldrich and dried over molecular sieves before use. All dry solvents were stored under dinitrogen or argon in Young's flasks over 4 Å molecular sieves.

$^1H$ and $^{13}C$ NMR experiments were performed at ambient temperature using a Bruker Avance-300; $^1H$ and $^{13}C$ NMR chemical shifts are referenced internally to residual non-deuterated solvent resonances. $^{19}F$ NMR experiments were performed at ambient temperature using a Bruker Avance-400 and referenced internally to residual non-deuterated solvent resonances. All chemical shifts are reported in $\delta$ (ppm) and coupling constants in hertz (Hz). The following abbreviations have been used for multiplicities: s (singlet), d (doublet), t (triplet), q (quartet), sept (septet), br (broad), m (unresolved multiplet). Elemental analyses were performed externally by Stephen Boyer of London Metropolitan University, U.K., using a Carlo Erba Flash 2000 Organic Elemental Analyzer. Thermogravi-

**Received:** February 18, 2013
**Published:** April 15, 2013

   dx.doi.org/10.1021/ic400420h | *Inorg. Chem.* 2013, 52, 5515−5526

metric analyses (TGA) were performed using a Perkin-Elmer TGA 4000 Thermogravimetric Analyzer,

**Synthesis.** *Synthesis of $[MeZn(O_2CC_2F_5)]_n$ (1).* $C_2F_5COOH$ (0.66 g, 4.0 mmol) was added to a stirred solution of $Me_2Zn$ (2 mL of 2 M solution in hexane, 4.0 mmol) in hexane (10 mL) at −78 °C. The solution was stirred overnight while slowly warming up to room temperature, a white precipitate remained. The mixture was warmed to 50 °C, leaving a clear solution; crystals were obtained on slow cooling of the solution to room temperature (0.61 g, 63%, mp 115−116 °C). Analysis found (calc. for $C_4H_3F_5O_2Zn$): C 19.8 (19.8), H 1.2 (1.3) %. $^1$H NMR (300 MHz, THF-$d^8$) $\delta$ ppm: −0.81 (s, 3H, $CH_3$), $^{13}$C NMR (300 MHz, $CDCl_3$) $\delta$ ppm: 163.2 (br. s, $CO_2$), 119.8 (qt, $J$ = 286.6, 35.4 Hz, $CF_3$), 108.0 (tq, $J$ = 264.2, 37.2 Hz, $CF_2$), −18.2 (br. s, $CH_3$), $^{19}$F NMR (400 MHz, THF-$d^8$) $\delta$ ppm: −85.7 (br. s, $CF_3$), −123.0 (br. s, $CF_2$).

*Synthesis of $Zn_{10}Me_4(OMe)_4(O_2CC_2F_5)_{12}$ (2).* Initial attempts to recrystallize **1** with the addition of $CH_2Cl_2$ (10 mL) and cooling to 5 °C produced **2** (0.38 g, 41%, mp 81−83 °C). Analysis found (calc. for $C_{22}H_{12}F_{30}O_{14}Zn_5$): C 19.3 (19.0), H 1.0 (0.9) %. $^1$H NMR (300 MHz, THF-$d^8$) $\delta$ ppm: 3.44 (br. s, 3H, $OCH_3$), −0.81 (s, 3H, $ZnCH_3$), $^{13}$C NMR (300 MHz, $CDCl_3$) $\delta$ ppm: 163.7 (br. s, $CO_2$), 119.8 (qt, $J$ = 285.9, 36.6 Hz, $CF_3$), 108.0 (tq, $J$ = 262.4, 37.8 Hz, $CF_2$), 53.8 (br. s, $OCH_3$), −18.2 (br. s, $CH_3$), $^{19}$F NMR (400 MHz, THF-$d^8$) $\delta$ ppm: −83.8 (s, $CF_3$), −121.2 (s, $CF_2$).

*Synthesis of $[MeZn(O_2CC_3F_7)]_n$ (3).* Prepared using the same synthesis method as for **1** using $C_3F_7COOH$ (0.86 g, 4.0 mmol) and $Me_2Zn$ (2 mL of 2 M solution in hexane, 4.0 mmol); yield 0.72 g, 62%, mp 81−83 °C. Analysis found (calc. for $C_5H_3F_7O_2Zn$): C 20.5 (20.6), H 1.2 (1.0) %. $^1$H NMR (300 MHz, THF-$d^8$) $\delta$ ppm: −0.80 (s, 3H, $CH_3$), $^{13}$C NMR (300 MHz, $CDCl_3$) $\delta$ ppm: 165.5 (br. s, $CO_2$), 119.0 (qt, $J$ = 288.2, 34.3 Hz, $CF_3$), 109.8 (tsxt, $J$ = 266.3, 34.3, $CF_2CF_3$), 109.6 (tt, $J$ = 265.3, 33.30 Hz, $O_2CCF_2$), −18.4 (br. s, $CH_3$), $^{19}$F NMR (500 MHz, $CDCl_3$) $\delta$ ppm: −82.4 (br. s, $CF_3$), −119.1 (br. s, $CF_2$), −128.3 (br. s, $CF_2$).

*Synthesis of $Zn_{10}Me_4(OMe)_4(O_2CC_3F_7)_{12}$ (4).* Initial attempts to recrystallize **3** with the addition of $CH_2Cl_2$ (10 mL) and cooling to 5 °C produced **4**; yield 0.41 g, 36%, mp 141−142 °C. Analysis found (calc. for $C_{28}H_{12}F_{42}O_{14}Zn_5$): C 19.8 (19.9), H 0.8 (0.7) %. $^1$H NMR (300 MHz, THF-$d^8$) $\delta$ ppm: 3.52 (br. s, 3H, $OCH_3$), −0.84 (s, 3H, $ZnCH_3$) $^{13}$C NMR (300 MHz, $CDCl_3$) $\delta$ ppm: 162.5 (br. s, $CO_2$), 117.5 (qt, $J$ = 286.6, 34.7 Hz, $CF_3$), 108.3 (tsxt, $J$ = 266.1, 39.1 Hz, $CF_2CF_3$), 108.2 (tt, $J$ = 267.3, 32.9 Hz, $O_2CCF_2$), 52.2 (br. s, $OCH_3$), −6.1 (s, $ZnCH_3$), $^{19}$F NMR (400 MHz, THF-$d^8$) $\delta$ ppm: −81.8 (s, $CF_3$), −118.5 (br. s, CF2), −127.9 (s, $CF_2$).

*Synthesis of $[EtZn(O_2CC_2F_5)]_n$ (5).* Prepared using the same synthesis method as for **1** using $C_2F_5COOH$ (0.66 g, 4.0 mmol) and $Et_2Zn$ (4 mL of 1 M solution in hexane, 4.0 mmol), leaving a clear solution with a small amount of white precipitate. Crystals were obtained on filtering the solution and cooling to −20 °C (0.71 g, 70%, mp 89−91 °C). Analysis found (calc. for $C_5H_5F_5O_2Zn$): C 23.6 (23.4), H 1.9 (2.0) %. $^1$H NMR (500 MHz, THF-$d^8$) $\delta$ ppm: 1.17 (t, $J$ = 8.04 Hz, 3H, $CH_3$), 0.21 (q, $J$ = 8.20 Hz, 2H, $CH_2$), $^{13}$C NMR (500 MHz, THF-$d^8$) $\delta$ ppm: 164.1 (br. s, $CO_2$), 119.7 (qt, $J$ = 284.3, 34.5 Hz, $CF_3$), 108.0 (tq, $J$ = 264.3, 37.2 Hz, $CF_2$), 12.6 (s, $CH_3$), −2.7 (br. s, $CH_2$), $^{19}$F NMR (500 MHz, THF-$d^8$) $\delta$ ppm: −83.9 (br. s, $CF_3$), −121.2 (br. s, $CF_2$).

*Synthesis of $Zn_9Et_2(O_2CC_2F_5)_{12}(O)_2$ (6).* From synthesis of **5**, the small amount of white precipitate was dissolved in $CH_2Cl_2$ (10 mL) and hexane (10 mL), the solution was filtered, and colorless crystals were obtained on cooling to 5 °C (0.09 g, 10%, mp 134−136 °C). Analysis found (calc. for $C_{40}H_{10}F_{60}O_{26}Zn_9$): C 18.2 (18.3), H 0.5 (0.4) %.

*Synthesis of $[EtZn(O_2CC_3F_7)]_n$ (7).* Prepared using the same synthesis method as for **1** using $C_3F_7COOH$ (0.86 g, 4.0 mmol) and $Et_2Zn$ (4 mL of 1 M solution in hexane, 4.0 mmol); yield 0.79 g, 65%, mp 96−99 °C. Analysis found (calc. for $C_6H_5F_7O_2Zn$): C 22.6 (23.5), H 1.6 (1.7) %. $^1$H NMR (300 MHz, THF-$d^8$) $\delta$ ppm: 1.17 (t, $J$ = 7.91 Hz, 3H, $CH_3$), 0.21 (q, $J$ = 8.10 Hz, 2H, $CH_2$), $^{13}$C NMR (500 MHz, $CDCl_3$) $\delta$ ppm: 162.9 (br. s, $CO_2$), 119.1 (qt, $J$ = 288.0, 33.4 Hz, $CF_3$), 109.8 (tsxt, $J$ = 264.2, 35.3 Hz, $CF_2CF_3$), 109.6 (tt, $J$ = 264.2, 35.5 Hz, $CF_2CF_2CF_3$), 12.6 (s, $CH_3$), −2.8 (s, $CH_2$), $^{19}$F NMR (500 MHz, $CDCl_3$) $\delta$ ppm: −81.8 (br. s, $CF_3$), −118.4 (br. s, $CF_2$), −127.8 (br. s, $CF_2$).

*$Zn_8Et_4(OEt)_4(O_2CC_3F_7)_6(O)$ (8).* Initial attempts to recrystallize **7** with the addition of $CH_2Cl_2$ (10 mL) and cooling to 5 °C produced **8** (0.43 g, 41%, mp 115−117 °C). Analysis found (calc. for $C_{40}H_{40}F_{42}O_{17}Zn_8$): C 22.7 (22.8), H 1.9 (1.9) %. $^1$H NMR (300 MHz, $CDCl_3$) $\delta$ ppm: 3.74 (q, $J$ = 7.03 Hz, 2H, $OCH_2$), 1.07 (t, $J$ = 7.20 Hz, 3H, $OCH_2CH_3$), 0.96 (t, $J$ = 7.90 Hz, 3H, $ZnCH_2CH_3$), −0.01 (q, $J$ = 7.91 Hz, 2 H, $ZnCH_2$), $^{13}$C NMR (300 MHz, $CDCl_3$) $\delta$ ppm: 165.0 (br. s, $CO_2$), 119.1 (qt, $J$ = 286.1, 36.2 Hz, $CF_3$), 109.9 (tsxt, $J$ = 266.1, 36.2, Hz, $CF_2CF_3$), 109.8 (tt, $J$ = 267.0, 34.3 Hz, $CF_2CF_2CF_3$), 63.7 (br. s., $OCH_2$), 21.3 (br. s., $OCH_2CH_3$), 12.7 (s, $ZnCH_2CH_3$), −2.51 (br. s., $ZnCH_2$), $^{19}$F NMR (400 MHz, THF-$d^8$) $\delta$ ppm: −81.8 (s, $CF_3$), −118.5 (br. s, CF2), −127.8 (s, $CF_2$).

*Synthesis of $MeZn(O_2CC_2F_5)TMEDA$ (9).* $C_2F_5COOH$ (0.65 g, 4.0 mmol) was added to a stirred solution of $Me_2Zn$ (3 mL of 2 M solution in hexane, 6.0 mmol) and TMEDA (0.47g, 4.0 mmol) in hexane (10 mL) at −78 °C. Solution was stirred overnight while slowly warming up to room temperature. Solvent and volatiles were removed in vacuo, a colorless oil remained (0.94 g, 66%, mp 119−120 °C). Analysis found (calc. for $C_{10}H_{19}F_5N_2O_2Zn$): C 33.4 (33.5), H 5.3 (5.4), N 7.7 (7.8) %. $^1$H NMR (300 MHz, THF-$d^8$) $\delta$ ppm: 2.68 (s, 4H, $NCH_2$), 2.44 (s, 12H, $NCH_3$), −0.93 (s, 3H, $ZnCH_3$), $^{13}$C NMR (300 MHz, THF-$d^8$) $\delta$ ppm: 161.6 (t, $J$ = 24.8 Hz, $CO_2$), 120.2 (qt, $J$ = 285.9, 36.0 Hz, $CF_3$), 108.1 (tq, $J$ = 260.5, 36.6 Hz, $CF_2$), 57.7 (s, $NCH_2$), 46.9 (s, $NCH_3$), −18.7 (s, $ZnCH_3$), $^{19}$F NMR (400 MHz, THF-$d^8$) $\delta$ ppm: −85.5 ($CF_3$), −122.7 ($CF_2$).

Also prepared by the same method:

*$MeZn(O_2CC_3F_7)TMEDA$ (10).* Using $C_3F_7COOH$ (0.86 g, 4.0 mmol), $Me_2Zn$ (3 mL of 2 M solution in hexane, 6.0 mmol), and TMEDA (0.47 g, 4.0 mmol); yield 1.42 g, 87%, mp 97−99 °C. Analysis found (calc. for $C_{11}H_{19}F_7N_2O_2Zn$): C 32.2 (32.4), H 4.5 (4.7), N 6.9 (6.9) %. $^1$H NMR (300 MHz, THF-$d^8$) $\delta$ ppm: 2.69 (s, 4H, $NCH_2$), 2.45 (s, 12H, $NCH_3$), −0.93 (s, 3H, $ZnCH_3$), $^{13}$C NMR (500 MHz, THF-$d^8$) $\delta$ ppm: 161.7 (t, 25.1 Hz, $CO_2$), 119.3 (qt, $J$ = 286.6, 33.8 Hz, $CF_3$), 110.2 (tsxt, $J$ = 264.8, 36.0 Hz, $CF_2CF_3$), 109.8 (tt, $J$ = 263.8, 31.6 Hz, $O_2CCF_2$), 57.8 (s, $NCH_2$), 47.0 (s, $NCH_3$), −18.7 (s, $ZnCH_3$), $^{19}$F NMR (400 MHz, THF-$d^8$) $\delta$ ppm: −83.6 ($CF_3$), −119.9 ($CF_2$), −129.4 ($CF_2$).

*$EtZn(O_2CC_2F_5)TMEDA$ (11).* Using $C_2F_5COOH$ (0.65 g, 4.0 mmol), $Et_2Zn$ (6 mL of 1 M solution in hexane, 6.0 mmol), and TMEDA (0.47 g, 4.0 mmol); yield 1.36 g, 91%. On standing, crystals formed in oil. Analysis found (calc. for $C_{11}H_{21}F_5N_2O_2Zn$): C 35.3 (35.5), H 5.6 (5.7), N 7.5 (7.5) %. $^1$H NMR (300 MHz, THF-$d^8$) $\delta$ ppm: 2.68 (s, 4H, $NCH_2$), 2.45 (s, 12H, $NCH_3$), 1.18 (t, $J$ = 8.10 Hz, 3H, $ZnCH_2CH_3$), 0.10 (q, $J$ = 8.30 Hz, 2H, $ZnCH_2CH_3$), $^{13}$C NMR (300 MHz, THF-$d^8$) $\delta$ ppm: 162.2 (t, 26.1 Hz, $CO_2$), 120.2 (qt, $J$ = 284.7, 34.7 Hz, $CF_3$), 108.2 (tq, $J$ = 262.4, 37.2 Hz, $CF_2$), 57.8 (s, $NCH_2$), 47.1 (s, $NCH_3$), 13.4 (s, $ZnCH_2CH_3$), −3.3 (s, $ZnCH_2CH_3$), $^{19}$F NMR (400 MHz, THF-$d^8$) $\delta$ ppm: −85.5 ($CF_3$), −122.6 ($CF_2$).

*$EtZn(O_2CC_3F_7)TMEDA$ (12).* Using $C_3F_7COOH$ (0.86 g, 4.0 mmol), $Et_2Zn$ (6 mL of 1 M solution in hexane, 6.0 mmol), and TMEDA (0.47 g, 4.0 mmol); yield 1.51 g, 89%. Analysis found (calc. for $C_{12}H_{21}F_7N_2O_2Zn$): C 33.9 (34.1), H 4.9 (5.0), N 6.5 (6.4) %. $^1$H NMR (300 MHz, THF-$d^8$) $\delta$ ppm: 2.68 (s, 4H, $NCH_2$), 2.46 (s, 12H, $NCH_3$), 1.18 (t, $J$ = 8.10 Hz, 3H, $ZnCH_2CH_3$), 0.09 (q, $J$ = 8.30 Hz, 2H, $ZnCH_2CH_3$), $^{13}$C NMR (500 MHz, THF-$d^8$) $\delta$ ppm: 161.6 (t, $J$ = 24.5 Hz, $CO_2$), 119.3 (qt, $J$ = 287.0, 34.5 Hz, $CF_3$), 110.2 (tsxt, $J$ = 264.3, 36.1 Hz, $CF_2CF_3$), 108.2 (tt, $J$ = 264.3, 30.9 Hz, $O_2CCF_2$), 57.8 (s, $NCH_2$), 47.1 (s, $NCH_3$), 13.3 (s, $ZnCH_2CH_3$), −3.3 (s, $ZnCH_2CH_3$), $^{19}$F NMR (400 MHz, THF-$d^8$) $\delta$ ppm: −83.6 ($CF_3$), −119.8 ($CF_2$), −122.6 ($CF_2$)

*Synthesis of $[Zn(O_2CC_2F_5)_2TMEDA]_2$ (13).* $C_2F_5COOH$ (1.32 g, 8.0 mmol) was added to a stirred solution of $Et_2Zn$ (4 mL of 1 M solution in hexane, 4.0 mmol) and TMEDA (0.47 g, 4.0 mmol) in hexane (10 mL) at −78 °C. Solution was stirred overnight while slowly warming up to room temperature. Solvent and volatiles were removed in vacuo, and a white solid remained. Solid was redissolved in THF (5 mL), and colorless crystals were obtained on cooling to −20 °C (1.74 g, 86%,


dx.doi.org/10.1021/ic400420h | Inorg. Chem. 2013, 52, 5515−5526

**Table 1. Crystal Data and Structure Refinement for 2, 5−8, 11, 13, 15**

| | 2 | 5 | 6 | 7 | 8 | 11 | 13 | 15 |
|---|---|---|---|---|---|---|---|---|
| empirical formula | $C_{44}H_{24}F_{60}O_{28}Zn_{10}$ | $C_{10}H_{10}F_{10}O_4Zn_2$ | $C_{40}H_{10}F_{60}O_{26}Zn_9$ | $C_6H_5F_7O_2Zn$ | $C_{40}H_{40}F_{42}O_{17}Zn_8$ | $C_{11}H_{21}F_5N_2O_2Zn$ | $C_{24}H_{32}F_{20}N_4O_8Zn_2$ | $C_{28}H_{34}F_{28}N_4O_9Zn_2$ |
| formula weight | 2794.33 | 514.92 | 2634.81 | 307.47 | 2113.68 | 373.67 | 1015.28 | 1233.33 |
| crystal system | monoclinic | triclinic | monoclinic | monoclinic | orthorhombic | monoclinic | orthorhombic | triclinic |
| space group | $P2_1/n$ | $P\bar{1}$ | $C2/c$ | $C2/c$ | $P22_12_1$ | $P2_1/n$ | $Pc2_1b$ | $P\bar{1}$ |
| $a$ (Å) | 10.3599(4) | 9.5320(7) | 20.1556(5) | 19.1655(8) | 13.260(2) | 8.5671(2) | 12.6211(2) | 9.7929(2) |
| $b$ (Å) | 20.8103(10) | 9.7246(6) | 17.4860(5) | 10.4966(4) | 13.903(2) | 15.6795(5) | 16.2796(2) | 15.4901(3) |
| $c$ (Å) | 19.4299(10) | 10.1299(9) | 23.4712(5) | 10.0172(3) | 18.434(3) | 12.7444(3) | 19.1244(3) | 15.5496(4) |
| $\alpha$ (deg) | | 62.429(5) | | | | | | 95.574(1) |
| $\beta$ (deg) | 97.699(3) | 86.995(4) | 112.553(1) | 102.881(3) | | 109.487(1) | | 104.898(1) |
| $\gamma$ (deg) | | 88.439(4) | | | | | | 96.891(1) |
| $V$ (Å$^3$) | 4151.2(3) | 831.21(11) | 7639.6(3) | 1964.47(13) | 3398.5(9) | 1613.86(7) | 3929.42(10) | 2242.78(9) |
| $Z$ | 2 | 2 | 4 | 8 | 2 | 4 | 4 | 2 |
| $\rho_{calc}$ (mg m$^{-3}$) | 2.236 3 | 2.057 | 2.291 | 2.079 | 2.066 | 1.538 | 1.716 | 1.826 |
| $\mu$(Mo-K$_\alpha$) (mm$^{-1}$) | 3.041 | 3.004 | 2.992 | 2.589 | 2.947[1] | 1.577 | 1.362 | 1.237 |
| $F$(000) | 2704 | 504 | 5072 | 1200 | 2068 | 768 | 2032 | 1228 |
| crystal size (mm) | 0.10 × 0.10 × 0.10 | 0.45 × 0.20 × 0.10 | 0.15 × 0.10 × 0.05 | 0.45 × 0.10 × 0.10 | 0.20 × 0.20 × 0.15 | 0.40 × 0.35 × 0.25 | 0.50 × 0.50 × 0.40 | 0.30 × 0.30 × 0.30 |
| $\theta$ range (deg) | 3.62−25.03 | 5.18−24.97 | 3.68−27.51 | 3.21−27.46 | 3.58−27.46° | 4.35−27.49 | 4.61−27.45 | 2.94−27.54 |
| refl'ns collected | 41678 | 7439 | 65172 | 17749 | 26448 | 20503 | 52992 | 45149 |
| independent refl'ns [$R$(int)] | 7213 [0.3187] | 2874 [0.0627] | 8731 [0.1223] | 2238 [0.0503] | 7744 [0.0808] | 3677 [0.0376] | 8910 [0.0515] | 10254 [0.0619] |
| refle'ns observed (>2$\sigma$) | 4200 | 2321 | 4916 | 1752 | 5934 | 3177 | 7608 | 6782 |
| data completeness | 0.982 | 0.984 | 0.993 | 0.996 | 0.994 | 0.992 | 0.992 | 0.990 |
| max min trans | | 0.7532, 0.3450 | 0.8648, 0.6624 | 0.7818, 0.3887 | 0.5533, 0.3412 | 0.6939, 0.5712 | 0.6118, 0.5491 | 0.7078, 0.7078 |
| goodness-of-fit on $F^2$ | 1.073 | 1.063 | 1.021 | 1.052 | 1.074 | 1.084 | 1.037 | 1.018 |
| final R$_1$, wR$_2$ [I > 2$\sigma$(I)] | 0.0736, 0.1702 | 0.0831, 0.2256 | 0.0569, 0.0978 | 0.0317, 0.0729 | 0.0748, 0.1999 | 0.0303, 0.0712 | 0.0374, 0.0941 | 0.0472, 0.1073 |
| final R$_1$, wR$_2$ (all data) | 0.1422,0.2132 | 0.0982, 0.2430 | 0.1310, 0.1210 | 0.0503, 0.0808 | 0.0934, 0.2114 | 0.0381, 0.0769 | 0.0487, 0.1027 | 0.0890, 0.1254 |
| largest diff. peak, hole (eÅ$^{-3}$) | 1.081, −1.113 | 3.859, −1.026 | 0.650, −0.609 | 0.472, −0.571 | 3.035, −1.103 | 0.384, −0.372 | 0.424, −0.376 | 0.917, −0.708 |
| Flack parameter | | | | | 0.02(2) | | 0.007(11) | |



dx.doi.org/10.1021/ic400420h | Inorg. Chem. 2013, 52, 5515−5526

mp 97−99 °C). Analysis found (calc. for $C_{12}H_{16}F_{10}N_2O_4Zn$): C 28.3 (28.4), H 3.1(3.2), N 5.5 (5.5) %. $^1$H NMR (300 MHz, THF-$d^8$) $\delta$ ppm: 2.73 (s, 4H, $NCH_2$), 2.50 (s, 12H, $NCH_3$), $^{13}$C NMR (300 MHz, THF-$d^8$) $\delta$ ppm: 162.7 (t, $J$ = 26.7 Hz, $CO_2$), 119.8 (qt, $J$ = 285.9, 34.7 Hz, $CF_3$), 108.1 (tq, $J$ = 263.0, 37.8 Hz, $CF_2$), 57.5 (s, $NCH_2$), 46.8 (s, $NCH_3$), $^{19}$F NMR (400 MHz, THF-$d^8$) $\delta$ ppm: −85.7 ($CF_3$), −123.1 ($CF_2$)

Also prepared by the same method:

*[Zn($O_2CC_3F_7$)$_2$TMEDA]$_2$ (**14**).* Using $C_3F_7COOH$ (1.71 g, 8.0 mmol), $Et_2Zn$ (4 mL of 1 M solution in hexane, 4.0 mmol), and TMEDA (0.47 g, 4 mmol); yield 2.05 g, 85%, mp 119−120 °C. Analysis found (calc. for $C_{14}H_{16}F_{14}N_2O_4Zn$): C 27.8 (27.7), H 2.5 (2.7), N 4.7 (4.6) %. $^1$H NMR (500 MHz, THF-$d^8$) $\delta$ ppm: 2.72 (s, 4H, $NCH_2$), 2.49 (s, 12H, $NCH_3$). $^{13}$C NMR (500 MHz, THF-$d^8$) $\delta$ ppm: 162.8 (br. s, $CO_2$), 119.1 (qt, $J$ = 287.0, 34.5 Hz, $CF_3$), 110.0 (tsxt, $J$ = 266.1, 36.1 Hz, $CF_2CF_3$), 109.8 (tt, $J$ = 265.2, 37.1 Hz, $O_2CCF_2$), 57.7 (s, $NCH_2$), 47.0 (s, $NCH_3$), $^{19}$F NMR (500 MHz, THF-$d^8$) $\delta$ ppm: −83.8 (t, $J$ = 8.67 Hz, $CF_3$), −120.6 (br. s, $CF_2$), −129.6 (s, $CF_2$).

Recrystallization of **14** from THF produced a few crystals of the hydrated species [Zn($O_2CC_3F_7$)$_2$·TMEDA]$_2$·$H_2O$ (**15**), which has been characterized solely by X-ray crystallography.

**Crystallography.** Experimental details relating to the single-crystal X-ray crystallographic studies are summarized in Table 1. For all structures, data were collected on a Nonius Kappa CCD diffractometer at 150(2) K using Mo−$K_\alpha$ radiation ($\lambda$ = 0.71073 Å). Structure solution was followed by full-matrix least-squares refinement and was performed using the WinGX-1.70 suite of programmes.[23] There were several issues with the structure determinations, specifically associated with disorder in the fluorocarbon groups, details of which are given below; in no case is the overall structure compromised by the difficulties in addressing these disorders.

In **2**, there are two $Zn_5$ units linked through an inversion center at the heart of the dimer. Two of the $C_2F_5$ groups show disorder, one in the ratio 50:50 and the other in the ratio 70:30; two internuclear distances [C(4)-F(2) and C(7)-F(7A)] have been restrained.

Difficulties in solving and refining the structure of **8** were concentrated at the "determination of space group". The absences recorded were indicative of 3 possibilities, namely, $Pnm2_1$, $Pn21m$, and $Pnmm$, none of which afforded a reasonable starting point. Ultimately, the structure was solved in a low symmetry space group, and the location of the motif used to establish the correct assignment ($P22_12_1$) as presented herein. The employment of special positions invoked in the model, give rise to a special absence—in this case the "$n$" glide—which is not "real". Refinement was uneventful, and residual electron density is chemically insignificant, being a ripple close to one of the zinc atoms in the aggregate that constitutes the core of this compound.

In **13** there is disorder in two out of the four $C_2F_5$ groups in the ratio 1:1. There is potential disorder in one more $C_2F_5$ group; however, it was not possible to resolve this; in particular, C(21) has a very large ADP and could potentially be split into two positions, but attempts to effect this resulted in divergent refinement. All internuclear distances in the disordered groups have been idealized and some of the ADPs equalized.

In **15** there is disorder in two of the four $C_3F_7$ groups in the ratio 60:40. All C−C and some C−F internuclear distances in the disordered $C_3F_7$ group based on C(31)−C(34) have been restrained. The hydrogen atoms of the water ligand have been located in the difference Fourier map and freely refined.

**Materials Chemistry.** TGA of the complexes was performed using a Perkin-Elmer TGA 4000 Thermogravimetric Analyzer. Data points were collected every second at a ramp rate of 5 °C min$^{-1}$ in a flowing (20 mL min$^{-1}$) $N_2$ stream. CVD was carried out on an ElectroGas Systems cold-walled reactor with associated gas lines and electronic heater controls. Specific conditions used for precursors **3**, **10**, **13** were as follows: **3**: Films were grown at 450 °C onto glass for 2 h with the line and bubbler temperatures set to 150 °C and a pressure of 47.2 Torr; **10**: Films were grown on glass substrates at a reactor temperature of 400 °C, with a line and bubbler temperature of 90 °C and a pressure of 39.6 Torr for a duration of 90 min; **13**: Films were grown on glass substrates at a reactor temperature of 450 °C and a bubbler and line temperature of 150 °C for 120 min at a pressure of 39.8 Torr. In all cases, there was a bleed of mixed $N_2$ (300 mL min$^{-1}$) and $O_2$ (60 mL min$^{-1}$) as carrier gas

## RESULTS AND DISCUSSION

**Synthesis and Structures.** Organozinc fluorocarboxylates were prepared following a literature method for the preparation of $EtZnO_2CPh$ (eq 1).[24] The resulting air- and moisture-sensitive white products were isolated and characterized by NMR, which are unexceptional save that they confirm the retention of one alkyl group on zinc and, from the $^{13}$C NMR, that the fluorocarbon residue remains intact; yields were in the range 61−70%.

$$R_2Zn + R_fCO_2H \xrightarrow[-78^\circ C,Ar,-RH]{\text{hexane}} (RZnO_2CR_f)_n$$
(**1**)R=Me,$R_f$=$C_2F_5$
(**3**)R=Me,$R_f$=$C_3F_7$
(**5**)R=Et,$R_f$=$C_2F_5$
(**7**)R=Et,$R_f$=$C_3F_7$ (1)

Initial attempts to recrystallize (**1**) and (**3**) by adding $CH_2Cl_2$ to the hexane solution and cooling to −5 °C produced two oxidation products, $Zn_{10}Me_4(OMe)_4(O_2CR_f)_{12}$ [$R_f$ = $C_2F_5$ (**2**); $C_3F_7$ (**4**)]. Both (**2**) and (**4**) showed $^1$H NMR resonances due to the different ZnMe and ZnOMe peaks with shifts of −0.81, 3.44 ppm (**2**) and −0.84, 3.52 ppm (**4**) in a 1: 1 ratio. The presence of OMe groups is consistent with a reaction of **1**, **3** with $O_2$, as the reaction between $O_2$ and dialkylzinc compounds is known to produce first zinc peroxides which then transform to the thermodynamically more stable alkoxides.[25−27]

Similarly, a small number of crystals of $Zn_9Et_2(O_2CC_2F_5)_{12}(O)_2$ (**6**) were obtained from dissolving the hexane insoluble precipitate left from the synthesis of **5** in a hexane/$CH_2Cl_2$ mixture and cooling to −20 °C, though the amount of material was sufficient only for crystallography and microanalysis. The inclusion of oxygen atoms within the cage could be plausibly attributed to two different mechanisms. Lewiński et al. have synthesized a similar cage, [Zn-($O_2CPh$)]$_4$O, on addition of dry $O_2$ to [$EtZn(O_2CPh)$]$_n$. They speculated that the mechanism starts with attack of $O_2$ on the Zn−C bond to form a peroxide, $EtOOZn(O_2CPh)$, which could then associate with any remaining [$EtZn(O_2CPh)$]$_n$ to form [$EtZn(O_2CPh)$]$_x$[$EtOOZn(O_2CPh)$]$_y$. Homolysis of the O−O bond then produces both alkoxyl and oxyzinc radicals, and the latter is the origin of the Zn−O−Zn moiety in the final product.[25,26] Alternatively, **6** could simply be a product from the hydrolysis of **5**. **6** can also be reformulated as $(EtZnL)_2(ZnL_2)_5(ZnO)_2$ (L = $O_2CC_2F_5$), and it is possible that in solution **5** undergoes Schlenk equilibria to form a mixture of $EtZnO_2CC_2F_5$, $Et_2Zn$, and $Zn(O_2CC_2F_5)_2$, with which a small amount of water in the solvent would hydrolyze $Et_2Zn$ to form ZnO which is trapped by the remaining species; Schlenk equilibria of this type are common for alkylzinc alkoxides.[26] The controlled hydrolysis of $EtZn_2(O_2CR)_3(THF)$ to form $Zn_4(O)(O_2CR)_6$ has recently been reported.[8]

Finally, $Zn_8Et_4(OEt)_4(O_2CC_3F_7)_6(O)$ (**8**) was obtained from initial attempts to recrystallize **7** from the addition of $CH_2Cl_2$ to the hexane solution and cooling to −20 °C. Although the structure itself is very different to that of **6** it is likely that a similar mechanism is involved in its formation, that is, reaction of 7 with either $O_2$ or water. The $^1$H NMR spectrum of **8** shows the EtZn and ZnOEt groups [$^1$H $\delta$ of


dx.doi.org/10.1021/ic400420h | Inorg. Chem. 2013, 52, 5515−5526

−0.01 (2H, $ZnCH_2$), 0.96 (3H, $ZnCH_2CH_3$), 1.07 (3H, $OCH_2CH_3$), and 3.74 ppm (2H, $OCH_2$)] while the $^{13}C$ NMR includes the expected coupling between $^{19}F$ and $^{13}C$ of the $R_f$ ligand.

To influence the volatility of the organozinc fluorocarboxylates, their synthesis was repeated in the presence of tetramethylethylenediamine (TMEDA) to attempt to break up the polymeric structures of the former (see below). Thus, 1:1 adducts **9**−**12** were synthesized in the reaction between $R_2Zn$ (R = Me, Et) and $R_fCO_2H$ ($R_f$ = $C_2F_5$,$C_3F_7$) in the presence of TMEDA in hexane, using a slight excess of $R_2Zn$ to ensure all the carboxylic acid reacted (eq 2). Volatiles were removed in vacuo, yielding the desired products as oils, though in the case of **11** this crystallized on standing over several days. $^1H$ NMR showed the correct 1:1 stoichiometry of alkylzinc species to TMEDA ligand.

$$1.5R_2Zn + R_fCO_2H + TMEDA \xrightarrow[-78^\circ C, Ar, -RH]{hexane} (RZnO_2CR_f).\ TMEDA$$
(**9**)R=Me,$R_f$=$C_2F_5$
(**10**)R=Me,$R_f$=$C_3F_7$
(**11**)R=Et,$R_f$=$C_2F_5$
(**12**)R=Et,$R_f$=$C_3F_7$ (2)

TMEDA adducts of zinc fluorocarboxylates $Zn(O_2CR_f)_2$·TMEDA were similarly synthesized from the reaction between $Et_2Zn$ and 2 equiv of fluorocarboxylic acid in the presence of TMEDA in hexane (eq 3). $^1H$ and $^{13}C$ NMR confirmed the presence of TMEDA and the carboxylate ligand, respectively.

$$Et_2Zn + 2R_fCO_2H + TMEDA \xrightarrow[-78^\circ C, Ar, -2RH]{hexane} Zn(O_2CR_f)_2TMEDA$$
(**13**)$R_f$=$C_2F_5$
(**14**)$R_f$=$C_3F_7$ (3)

Crystals of $[Zn(O_2CC_3F_7)_2$·TMEDA$]_2$·$H_2O$ (**15**) were also obtained on cooling a solution of **14** in THF to −20 °C over a period of 3 months.

*Structural Analysis.* The structures of $RZnO_2CR_f$ (R = Et, $R_f$ = $C_2F_5$ **5**, $C_3F_7$ **7**) have been determined and are essentially the same; a twinned crystal of **1** (R = Me, $R_f$ = $C_2F_5$) was also studied, and although a complete structure determination could not be completed, the data were sufficient to show that it also adopts the same structure as both **5** and **7**. Accordingly, only data for **7** is discussed here, with details for **5** available as Supporting Information.

The structure of $EtZnO_2CC_2F_7$ (**5**) (Figure 1) is that of a polymeric chain in which each carboxylate ligand bridges two zinc atoms. In addition, O(1) of the ligand bridges two zinc atoms in a $\mu_2$-manner, such that $[EtZnO_2CC_2F_5]_2$ dimers are joined via four-membered $Zn_2O_2$ rings. There is one long and one short Zn−O interaction, the shorter one involving the singly-bridging oxygen atoms [Zn−O(2): 1.9853(17) Å] with the longer Zn−O contacts belonging to the $\mu_2$-oxygen atoms [Zn−O(1): 2.1528(17), Zn−O(1′) 2.1634(16) Å]. Although zinc is nominally four-coordinate, bond angles around the metal lie in the range 77.40(7)−140.15(10)°, a degree of distortion which could be due to the close intermolecular contact with F(2) [2.789(16) Å]. This separation is longer than the sum of the covalent radii (2.04 Å) but shorter than the sum of the van der Waals radii (2.91 Å).

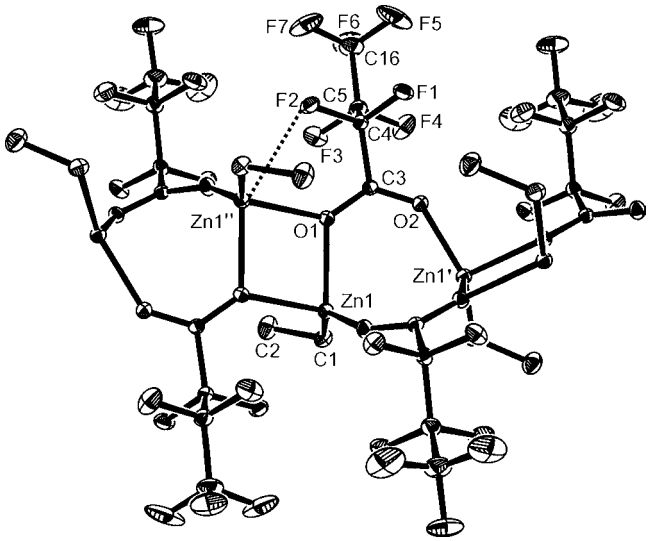


**Figure 1.** Asymmetric unit of **7** showing the labeling scheme used in the text and tables; thermal ellipsoids are at the 25% level. The figure shows a section of the polymer chain propagating along *c*. Selected geometric data: Zn−C(1) 1.939(3), Zn−O(1) 2.1528(17), Zn−O(2) 1.9853(17), Zn−O(1′) 2.1634(16), Zn···F(2) 2.789(16), O(1)−C(3) 1.262(3), O(2)−C(3) 1.237(3) Å; C(1)−Zn−O(1) 117.20(10), C(1)−Zn−O(2) 140.15(10), C(1)−Zn−O(1) 115.45(9), O(1)−Zn−O(2) 94.76(7), O(1)−Zn−O(1) 77.40(7), O(2)−Zn−O(1′) 93.26(7)°. Symmetry operations: ′ −*x*, *y*, 1/2 − *z*; ″ −*x*, −*y*, −*z*.

Four other $RZnO_2CR'$ structures free from additional donor groups have been reported which have lower degrees of oligomerization than those of **1**, **5**, **7**, namely, hexameric $EtZnO_2CPh$,[24] tetrameric $C_6F_5ZnO_2CR'$ (R′ = mesityl, 2-$ClC_6H_4$)[6] and dimeric when R is the extremely bulky *m*-terphenyl.[28] A more direct comparison can be made with the polymeric nature of $EtZnO_2CCH_3$[3] although here a sheet structure is adopted in which $Zn_2O_2$ rings are linked by 16-membered $[Zn(O_2CCH_3)]_4$ tetramers rather than the $[Zn(O_2CR_f)]_2$ dimers seen in **7** et al.

The simple $RZnO_2CR_f$ are very sensitive to either $O_2$ and/or $H_2O$, and react to yield the $Zn_{10}$ (**2**, **4**), $Zn_9$ (**6**), and $Zn_8$ (**8**) aggregated products. As far as we are aware, $Zn_7$ clusters, for example, $Zn_7(O)_2(O_2CMe)_{10}$(1-Meim)$_2$ (1-Meim = 1-methylimidazole)[29] are the largest comparable systems reported to date. Both **2** and **4** adopt the same $Zn_{10}Me_4(OMe)_4(O_2CR_f)_{12}$ formula, though disorder in the $C_3F_7$ groups in **4** hindered full structural determination, but it adopts the same framework as that of **2** (Figure 2).

The structure of **2** (Figure 2a) consists of a cage of five zinc atoms, surrounded by six bridging carboxylate ligands, two OMe groups, and two Me groups; one of the carboxylate ligands [based on C(18)] bridges to a symmetry-related second $Zn_5$ cage to yield an overall $Zn_{10}$ aggregate. Of the five zinc atoms, Zn(1) is in the center of the cage and is six-coordinated in a $ZnO_6$ environment, exhibiting a slightly distorted structure with bond angles ranging from 80.7(3)°−101.6(3)° between adjacent atoms and 168.1(3)°−174.7(3)° between opposite atoms. Of the remaining four zinc atoms, Zn(3) is five-coordinate $ZnO_5$ and Zn(2), Zn(4) and Zn(5) are all four-coordinate, though the first of these has $ZnO_4$ coordination and the latter pair bear methyl groups and are $ZnCO_3$ in ligation. A simplified view of the $Zn_5$ core is shown in Figure 2b.

Five-coordinate Zn(3) exhibits very distorted geometry ($\tau$ value of 0.42),[30] which is roughly half-way between square-


dx.doi.org/10.1021/ic400420h | *Inorg. Chem.* 2013, 52, 5515−5526

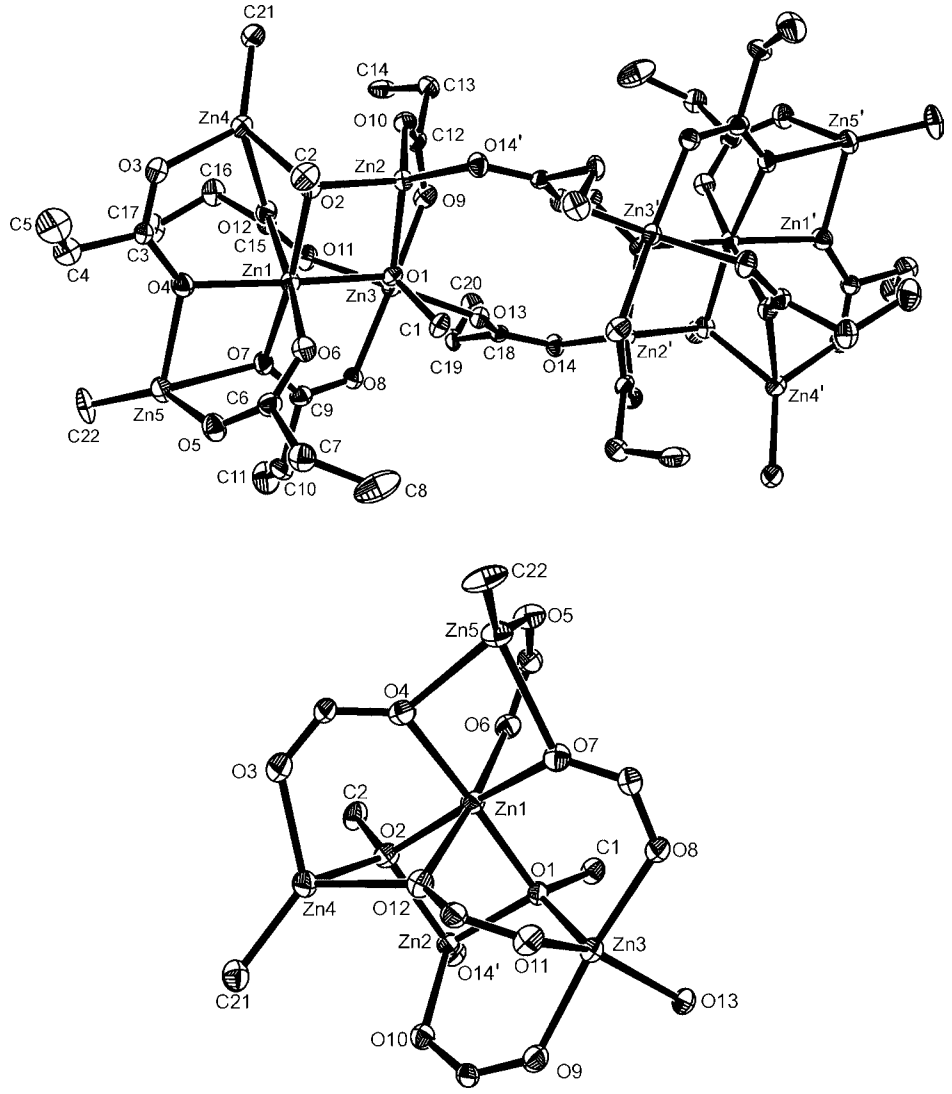


**Figure 2.** (a, top) Asymmetric unit of **2** showing the labeling scheme used in the text and tables and (b, bottom) a simplified view of the $Zn_5$ core; thermal ellipsoids are at the 25% level. Fluorine atoms have been removed for clarity. Selected internuclear distances: Zn(1)−O(1) 2.095(7), Zn(1)−O(2) 2.081(8), Zn(1)−O(4) 2.103(7), Zn(1)−O(6) 2.010(8), Zn(1)−O(7) 2.107(8), Zn(1)−O(12) 2.180(8), Zn(2)−O(1) 1.995(7), Zn(2)−O(2) 1.986(7), Zn(2)−O(10) 1.923(8), Zn(2)−O(14′) 1.932(7), Zn(3)−O(1) 2.023(7), Zn(3)−O(8) 2.056(8), Zn(3)−O(9) 2.071(9), Zn(3)−O(11) 2.035(7), Zn(3)−O(13) 2.014(7), Zn(4)−O(2) 2.090(7), Zn(4)−O(3) 2.026(8), Zn(4)−O(12) 2.207(8), Zn(4)−C(21) 1.931(13) Å. Symmetry operation: 1−*x*, −*y*, −*z*.

based pyramid and trigonal bipyramidal geometry. Zn(2), Zn(4), and Zn(5) all exhibit distorted tetrahedral geometry, with a much higher degree of distortion seen in Zn(4) and Zn(5), with bond angles ranging from 88.6(3)°−114.7(3)°, 76.2(3)°−129.7(4)°, and 75.9(3)°−143.6(5)°, respectively.

All the carboxylate groups bridge over at least two zinc atoms; of the six unique carboxylate ligands two bridge between zinc atoms within the $Zn_5$ unit [those based on C(6), C(12)], three have an additional $\mu_2$-link between two metals [i.e., coordinate three Zn in total; ligands based on C(3), C(9), and C(15)], while the final carboxylate [involving C(18)] bridges between $Zn_5$ moieties. The singly-bridging oxygen atoms have interatomic distances that are in the range 1.923(8) Å−2.071(9) Å while the $\mu_2$-oxygen atoms have slightly longer interatomic distances, ranging over 2.103(7) Å−2.258(7) Å. The oxygens of the OMe groups bridge in a $\mu_2$-mode over three zinc atoms, Zn(1), Zn(2), and Zn(3) in the case of O(1) and Zn(1), Zn(2), and Zn(4) in the case of O(2). The Zn−O interatomic distances range from 1.986(7) Å−2.095(7) Å, within the same range as the singly-bridging oxygen atoms of the carboxylate groups and slightly shorter than the $\mu_2$-oxygen atoms. Both Me groups are bonded to only one zinc atom each [Zn(4) and Zn(5)] and sit on the outskirts of the cage.

As far as we are aware, the $Zn_{10}$ frameworks of **2** and **4** are unique, but are clearly related to three known $Zn_5R_4(O_2CR')_6$ species (R = Et, R′ = Me;[31] R = $C_6F_5$, R′ = 2,4,6-$Me_3C_6H_2$, 3-$Me_2NC_6H_4$)[6] in that (i) there has been oxygen insertion into two Zn-R bonds of such species and (ii) the $Zn_5$ units in these compounds are now linked by one bridging carboxylate from each unit in **2**, **4**.

The nona-zinc species $Zn_9Et_2(O_2CC_2F_5)_{12}(O)_2$ (**6**) (Figure 3) contains a six-coordinate $ZnO_6$ [Zn(1)] which sits on an inversion center about which the cluster is built. **6** contains two other $ZnO_6$ moieties [Zn(4), Zn(4′)] and six four-coordinate zinc species, of which four have a $ZnO_4$ environment [Zn(2), Zn(3), and their symmetry-related partners] and two are $ZnCO_3$ species [Zn(5), Zn(5′)], which are the ethylzinc moieties at the two ends of the molecule. In contrast to **2** and **4**,


dx.doi.org/10.1021/ic400420h | *Inorg. Chem.* 2013, 52, 5515−5526

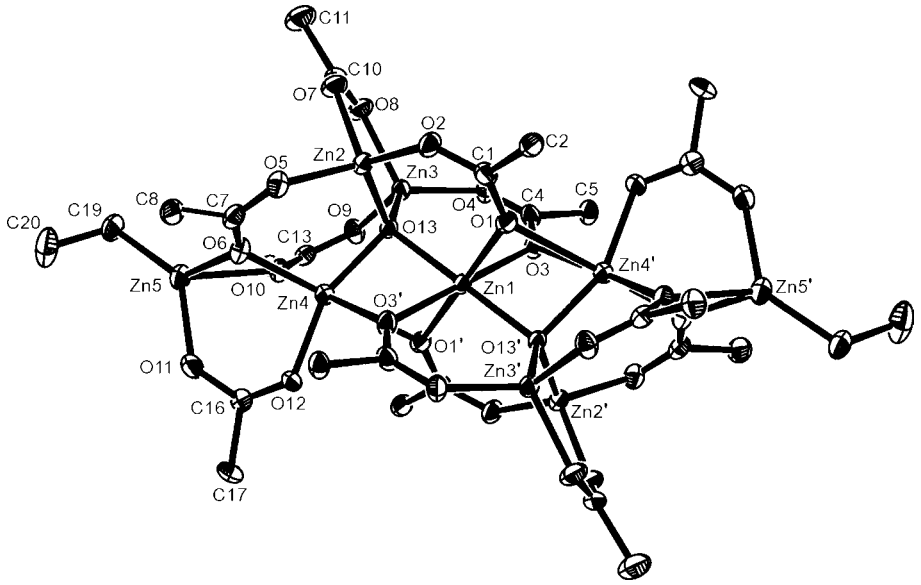


**Figure 3.** Asymmetric unit of **6** showing the labeling scheme used in the text and tables; thermal ellipsoids are at the 25% level. Only the $\alpha$-carbon of the $C_2F_5$ groups have been included for clarity; C(18) is hidden behind O(10). Selected internuclear distances: Zn(1)−O(1) 2.173(4), Zn(1)−O(3) 2.172(4), Zn(1)−O(13) 1.995(3), Zn(2)−O(2) 1.942(4), Zn(2)−O(3) 1.978(4), Zn(2)−O(7) 1.955(4), Zn(2)−O(13) 1.937(3), Zn(4)−O(1′) 2.423(4), Zn(4)−O(3) 2.454(4), Zn(4)−O(6) 2.108(4), Zn(4)−O(10) 2.101(4), Zn(4)−O(12) 1.938(4), Zn(4)−O(13) 1.940(3), Zn(5)−O(6) 2.270(4), Zn(5)−O(10) 2.236(4), Zn(5)−O(11) 1.950(5), Zn(5)−C(19) 1.924(6) Å. Symmetry operation: 1−*x*, 1−*y*, 1−*z*.

the carboxylate groups in **6** are predominantly *O,O*-bridging between two zinc atoms with one end also acting in a $\mu_2$-manner generating Zn−O−Zn linkages [eight, based on C(1), C(4), C(7), C(13) and symmetry-related groups], while only four ligands act purely in an *O,O*-bridging mode [based on C(10), C(16) and their partners]. Finally, O(13) acts in a $\mu_4$-manner linking Zn(1)−Zn(4) inclusive. Of the two six-coordinate Zn atoms, Zn(1) exhibits a geometry which is much closer to a perfect octahedron with bond angles of 180.0° between opposite oxygen atoms and bond angles in the range 80.19(13)°−99.81(13)° between adjacent oxygen atoms. Zn(4) shows a much more distorted geometry for which the corresponding ranges of angles are 154.92(15)°−178.03(15)° and 74.36(13)°−103.57(14)°, respectively. Of the four-coordinate zinc atoms, Zn(5) shows much more distortion [bond angles range: 73.01(14)°−135.2(2)°] than either Zn(2) and Zn(3) [bond angles: 98.20(18)°−113.81(15)° and 99.31(18)°−113.78(15)°, respectively]. The singly-bridging oxygen atoms have Zn−O interatomic distances that are in the range 1.938(4) Å−1.983(4) Å, while the $\mu_2$-oxygen atoms have longer Zn−O interatomic distances [2.101(4)−2.454(4) Å]; the oxygen atom in the center of the molecule, O(13), bridges over four Zn atoms and has Zn−O interatomic distances that are within the same range as the singly-bridging carboxylate oxygen atoms [1.937(3) Å−1.995(3) Å].

The asymmetric unit of octa-zinc $Zn_8Et_4(OEt)_4(O_2CC_3F_7)_6(O)$ (**8**) (Figure 4) is one-half of the formula unit, the remainder generated by a 2-fold axis through the $\mu_4$-O(1) at the center of the cluster. The asymmetric unit of **8** comprises two five-coordinate $ZnO_5$ centers [Zn(1), Zn(2)] internal to the cluster and two four-coordinate $ZnCO_3$ units, which, as in **6**, are at the ends of the aggregate. In addition to the $\mu_4$-O(1), there are two $\mu_3$-OEt groups, two carboxylates which *O,O*-bridge and additionally link two metals in a $\mu_2$- manner through one oxygen [based on C(1), C(5)], and one carboxylate which is *O,O*-bridging only [based on C(9)]. Zn(1) and Zn(2) both adopt a distorted trigonal bipyramidal coordination and $\tau$ values[30] of 0.66 and 0.61, respectively. Zn(1) has two oxygens from the carboxylate groups in the axial positions [O(2) and O(7)] with one more carboxylate oxygen [O(3)], one oxygen from an OEt group [O(9)], and the central O(1) in the equatorial positions. Similarly, Zn(2) has O(4) and O(6) in axial positions, both from carboxylate groups, and the central O(1), O(8) from an OEt and O(5) from a carboxylate group in the equatorial positions. Zn(3) and Zn(4) are both four-coordinate with a distorted tetrahedral structure and bond angles ranging from 78.9(2)°−130.8 (5)° and 79.4(2)°−130.8(4)°, respectively. The singly-bridging oxygens all have similar Zn−O interatomic distances [2.005(6) Å−2.049(7) Å] and are similar to those involving the $\mu_3$-OEt ligands [1.975(6) Å−2.122(5) Å], while the $\mu_2$-oxygen atoms have longer Zn−O interatomic distances [2.111(6) Å−2.406(6) Å]. O(1) is in the center of the cage, bridging over four zinc atoms with the two shortest Zn−O interactions [1.955(4), 1.950(4) Å].

The structure of $EtZn(O_2CC_2F_5)\cdot$TMEDA **11** is monomeric in the solid state, with the carboxylate group showing monodentate coordination (Figure 5); the Zn−O(2) bond [3.1341(16) Å] is outside the sum of the respective van der Waals radii (2.91 Å). The ligands are arranged about the central Zn atom in a distorted tetrahedral arrangement, with bond angles ranging from 84.86(6)° [N(1)−Zn−N(2)] to 126.98(8)° [C(10)−Zn−O(1)]. The TMEDA group shows iso-bidentate coordination, with identical internuclear distances between zinc and the two nitrogen atoms. Interestingly, despite the monodentate coordination of the carboxylate group, the internuclear distances between C(1) and both oxygen atoms are very similar, which can be rationalized by the presence of a weak hydrogen bond between O(2) and a hydrogen atom from an adjacent molecule [H(6b′)]. The structure of $EtZn(O_2CMe)(C_5H_4N)$ has recently been determined[32] and differs from **11** by incorporating a bridging carboxylate and a monodentate *N*-donor, though the coordination number at zinc is constant at four across both species.


dx.doi.org/10.1021/ic400420h | *Inorg. Chem.* 2013, 52, 5515−5526

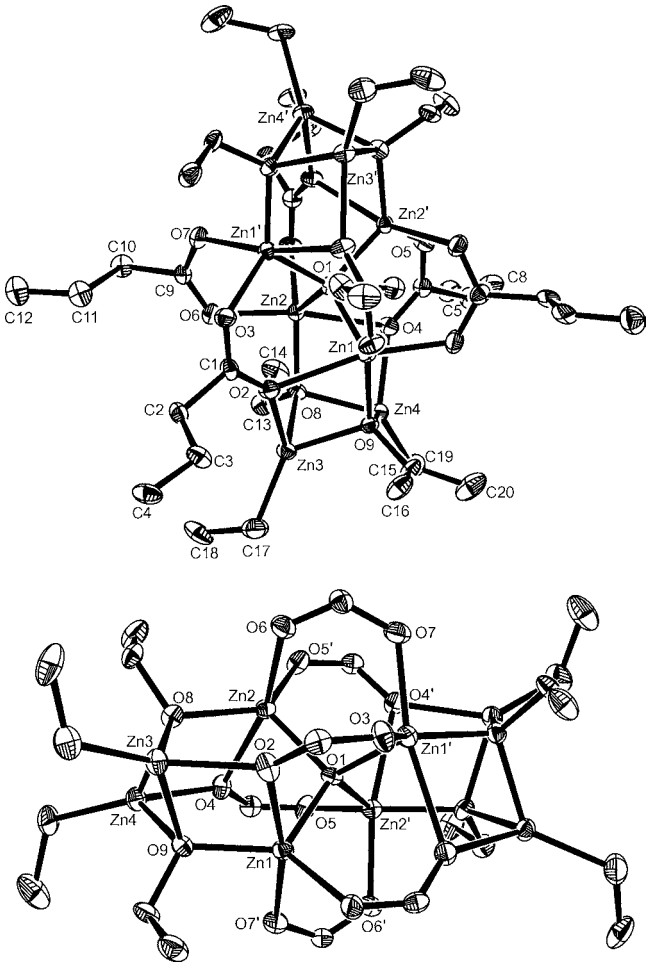


**Figure 4.** (a, top) Asymmetric unit of **8** showing the labeling scheme used in the text and tables; thermal ellipsoids are at the 25% level. Fluorine atoms have been removed for clarity; C(6) and C(7) are hidden by C(5); (b, bottom) the $Zn_8O_{17}$ core of **8**. Selected internuclear distances Zn(1)−O(1) 1.955(4), Zn(1)−O(2) 2.406(6), Zn(1)−O(3′) 2.017(6), Zn(1)−O(7′) 2.049(7), Zn(1)−O(9) 1.975(6), Zn(3)−O(2) 2.113(6), Zn(3)−O(8) 2.122(5), Zn(3)−O(9) 2.066(6), Zn(3)−C(17) 1.991(12) Å. Symmetry operation: *x*, 1−*y*, −*z*.

In contrast, $Zn(O_2CC_2F_5)\cdot$TMEDA (**13**) forms a dimer with four carboxylate ligands bridging between the two zinc atoms with the two TMEDA ligands capping each end of the dimer; both metals adopt a distorted octahedral $ZnO_4N_2$ coordination (Figure 6). All the carboxylate groups show bidentate coordination and in each case embody a short Zn−O to one metal and a longer, coordinate interaction with the other. There is a minor difference in the behavior of the two TMEDA ligands, with that bonded to Zn(1) doing so in an iso-bidentate manner, while the TMEDA bonded to Zn(2) has slight asymmetry in the Zn−N internuclear distances. Of compounds of the same generic composition, only the structure of $Zn(O_2CCH_3)_2\cdot$TMEDA appears to have been reported in literature and, in contrast to **13**, is monomeric with two aniso-bidentate acetate ligands and an iso-bidentate TMEDA ligand.[33]

Prolonged crystallization of $Zn(O_2CC_3F_7)\cdot$TMEDA (**14**) yielded small amounts of crystals of the hydrate, $[Zn(O_2CC_3F_7)\cdot TMEDA]\cdot H_2O$ (**15**), which adopts the same structure as $[Zn(O_2CCF_3)\cdot TMEDA]\cdot H_2O$ reported by

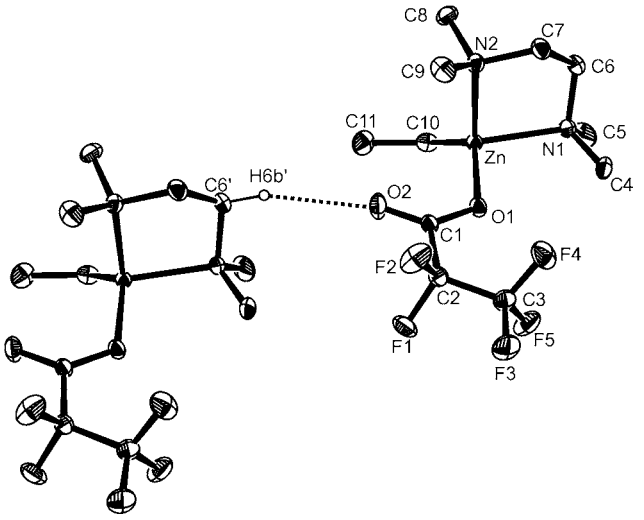


**Figure 5.** (a) Asymmetric unit of **11** showing the labeling scheme used in the text and tables; thermal ellipsoids are at the 25% level. Selected geometric data: Zn−C(10) 1.977(2), Zn−O(1) 2.0102(13), Zn−N(1) 2.1388(17), Zn−N(2) 2.1409(16), O(1)−C(1) 1.262(2), O2−C(1) 1.213(2) Å; C(10)−Zn−O(1) 126.98(8), C(10)−Zn−N(1) 120.15(9), C(10)−Zn−N(2) 119.12(8), O(1)−Zn−N(1) 96.22(6), O(1)−Zn−N(2) 99.12(8), N(1)−Zn−N(2) 84.86(6)°; O(2)−H-(6B′) 2.54, C(6)···O(2) 3.484(3) Å, ∠C(6′)−H(6B′)···O(2) 160 °. Symmetry operation: *x*−1, *y*, *z*.

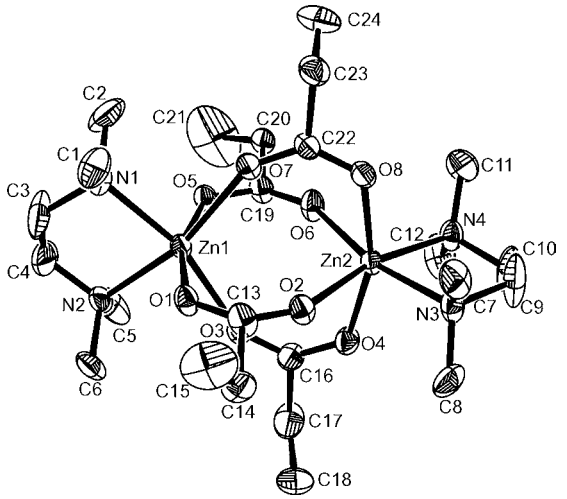


**Figure 6.** Asymmetric unit of **13** showing the labeling scheme used in the text and tables; thermal ellipsoids are at the 25% level. Fluorine atoms have been removed for clarity; Selected geometric data for Zn(1) as typical of the two metal atoms: Zn(1)−O(1) 1.978(2), Zn(1)−O(3) 2.134(3), Zn(1)−O(5) 1.972(2), Zn(1)−O(7) 2.350(3), O(1)−C(13) 1.241(5), O(2)−C(13) 1.223(5), O(3)−C(16) 1.220(5), O(4)−C(16) 1.249(5), Zn(1)−N(1) 2.185(3), Zn(1)−N(2) 2.199(3) Å; O(1)−Zn(1)−O(3) 84.82(12), O(1)−Zn(1)−O(5) 161.59(10), O(1)−Zn(1)−O(7) 85.02(11), O(1)−Zn(1)−N(1) 96.08(13), O(1)−Zn(1)−N(2) 98.31(12), O(3)−Zn(1)−O(5) 85.93(11), O(3)−Zn(1)−O(7) 113.71(9), O(3)−Zn(1)−N(1) 163.95(11), O(3)−Zn(1)−N(2) 80.99(12), O(5)−Zn(1)−O(7) 84.18(10), O(5)−Zn(1)−N(1) 97.20(13), O(5)−Zn(1)−N(2) 95.91(12), O(7)−Zn(1)−N(1) 82.32(12), O(7)−Zn(1)−N(2)165.23(12), N(1)−Zn(1)−N(2) 83.03(14)°.

others.[34] While the overall dimeric nature and $ZnO_4N_2$ coordination is retained from **13**, the presence of a molecule of water, which bridges in a $\mu_2$-manner between metals, causes


dx.doi.org/10.1021/ic400420h | Inorg. Chem. 2013, 52, 5515−5526

two of the carboxylate groups to become monodentate in **15** (Figure 7). In turn, these are then engaged in intramolecular

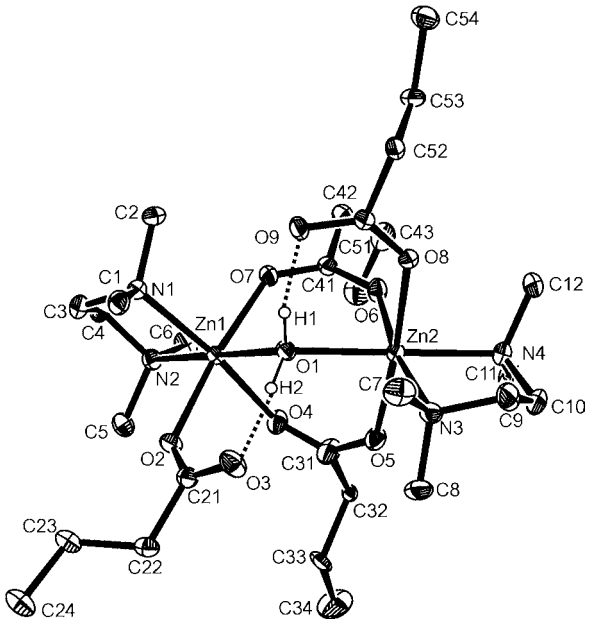


**Figure 7.** Asymmetric unit of **15** showing the labeling scheme used in the text and tables; thermal ellipsoids are at the 25% level. Fluorine atoms have been removed for clarity; C(44) is hidden behind O(6). Selected geometric data for Zn(1) as typical of the two metal atoms: Zn(1)−O(1) 2.184(2), Zn(1)−O(2) 2.143(2), Zn(1)−O(4) 2.089(2), Zn(1)−O(7) 2.097(2), O(2)−C(21) 1.253(4), O(3)−C(21) 1.237(4), O(4)−C(31) 1.230(4), O(5)−C(31) 1.238(4), Zn(1)−N(1) 2.181(3), Zn(1)−N(2) 2.159(3) Å; O(1)−Zn(1)−O(2) 86.99(9), O(1)−Zn(1)−O(4) 91.01(9), O(1)−Zn(1)−O(7) 87.40(9), O(1)−Zn(1)−N(2) 179.16(9), O(1)−Zn(1)−N(1) 96.02(9), O(2)−Zn(1)−O(4) 85.76(9), O(2)−Zn(1)−O(7) 173.14(8), O(2)−Zn(1)−N(1) 90.72(9), O(2)−Zn(1)−N(2) 93.60(9), O(4)−Zn(1)−O(7) 90.40(9), O(4)−Zn(1)−N(1) 171.98(9), O(4)−Zn(1)−N(2) 88.43(10), O(7)−Zn(1)−N(1) 93.79(9), O(7)−Zn(1)−N(2) 91.98(10), N(1)−Zn(1)−N(2) 84.59(10)°; H(2)−O(3) 1.72(5), ∠O(1)−H(2)···O(3) 169(4)°.

hydrogen bonding with the water molecule. The two bidentate carboxylate groups have very similar interatomic distances between the oxygen and the zinc, ranging from 2.078(2)−2.097(2) Å while the two monodentate carboxylate groups have slightly longer bonds [Zn(1)−O(2) 2.143(2), Zn(2)−O(8) 2.127(2) Å]; the water molecule which bridges between the two zinc atoms has even longer Zn−O internuclear distances [Zn(1)−O(1) [2.184(2), Zn(2)−O(1). 2.205(2) Å].

**Materials Chemistry.** TGA data for $RZnO_2CR_f$ complexes (**1**, **3**, **5**, **7**) are shown in Figure 8 and reveal quite different behavior for the species with $R_f = C_3F_7$ (**3**,**7**) to those with the shorter $C_2F_5$ function (**1**, **5**).

All four species show an initial weight loss of about 5% (R = Me) or 10% (R = Et), starting at about 130 °C, which are consistent with the loss of R (presumably as R-R or RH). Thereafter, both **1** and **5** undergo an ill-defined series of decomposition steps ultimately leaving a residue at about 430 °C of 30.5 and 38.9%, respectively; these values correspond most closely to either ZnO (33.0%) or $ZnF_2$ (39.9%) for **1**, **5**. The formation of $ZnF_2$ is plausible given the close intermolecular Zn···F contact seen in the solid-state structure (Supporting Information), analogous to that seen in **7** (Figure

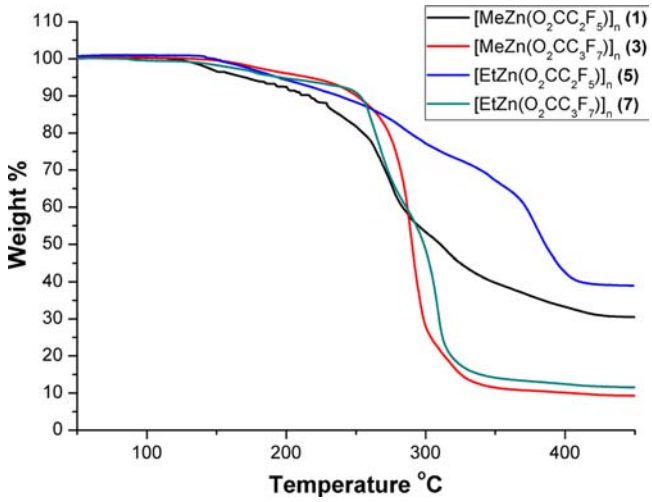


**Figure 8.** TGA data for $RZnO_2CR_f$ (**1**, **3**, **5**, **7**).

1), and the precedent for the formation of metal fluorides from, for example, metal fluoroalkoxides, under similar circumstances.[35] When a larger sample of **5** was heated to 400 °C under $N_2$, the temperature maintained for 1 h and then cooled to room temperature at 1 °C/min, the black residue (11.6% carbon impurity) that remained was shown to be tetragonal $ZnF_2$ by PXRD (Figure 9). While accurate quantitative EDX

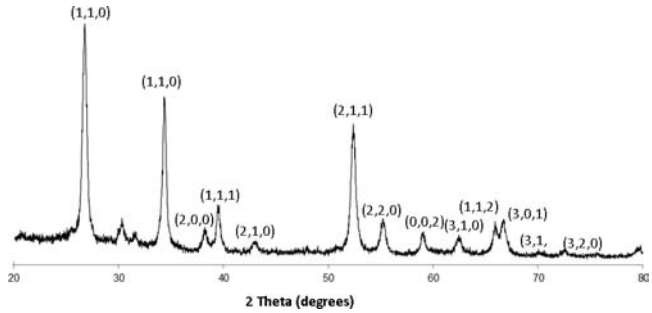


**Figure 9.** PXRD of the sample obtained by thermolysis of **5** under $N_2$ at 400 °C. The pattern is indexed to tetragonal $ZnF_2$ (PDF 89-5014).

analysis proved difficult because of sample charging, the atomic ratios broadly correspond to a mixture of largely $ZnF_2$ with a second, oxygen-containing species which is possibly Zn(OH)F, but there is no direct evidence for this in the PXRD (Figure 9) (EXD atomic % found: Zn 28.9, F 60.2, O 5.5; calc. for 0.18 Zn(OH)F + 0.82 $ZnF_2$ = Zn 31.4, F 57.2, O 5.7). Annealing in air converted the sample to a white crystalline material which EDX suggests contains only traces of fluorine (ca. 3.2 ± 1.7 atom %) and whose PXRD pattern can be indexed to ZnO (Supporting Information), with quantitative EDX approximating to $ZnO_{1.17}$ with negligible carbon contamination (<0.1%).

Compounds **3** and **7** undergo more clearly defined decomposition steps at $T$ > ca. 250 °C though we cannot make any rational assignments to these processes. The residues (9.3, 11.5% for **3**, **5**, respectively) are well below the values for either ZnO or $ZnF_2$ and strongly imply that these compounds are volatile.

**3** was chosen as the precursor for CVD trials because of its superior volatility; LPCVD (47.2 Torr) was the chosen technique as the precursor was not deemed volatile enough for APCVD. Films were grown at 450 °C onto glass over a


dx.doi.org/10.1021/ic400420h | Inorg. Chem. 2013, 52, 5515−5526

period of 2 h with the line and bubbler temperatures set to 150 °C. Films were transparent and did not conduct to any notable extent when tested with a voltammeter. SEM imaging (Figure 10a) reveals a uniform film consisting of crystallites of about

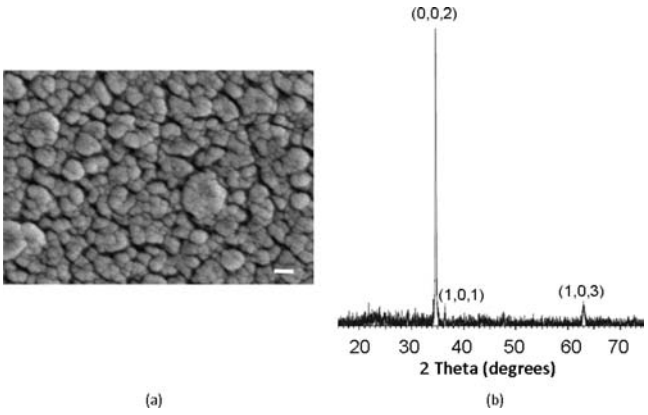


**Figure 10.** (a) SEM of the film grown from **3** by LPCVD, (b) PXRD of the film; indexing is to ZnO (PDF 89-1397); bar = 100 nm.

50−100 nm with cracks between clusters of these crystallites; EDX confirms the presence of Zn and O but could not detect any F in the film. PXRD confirms that a highly oriented ZnO film has been produced with a very intense peak corresponding to the (002) reflection (Figure 10b). The morphology of the ZnO crystallites does merit further comment. The common modification of ZnO thin films is usually as hexagonal rods, in which polar (001) faces are parallel to the substrate, that is, the *c*-axis and the substrate are parallel. In such a circumstance, the polar faces, which are commonly believed to be the active sites in various catalytic processes, are (i) in low abundance compared to the non-polar walls of the hexagon and (ii) largely inaccessible.[36,37] The growth of vertically-aligned hexagonal microplates, in which the (001) face (*c*-axis) is perpendicular to the substrate, have a larger surface area of available polar faces, and are seen to be more reactive, for example, enhanced photocatalytic activity.[38] The enhanced intensity of the (002) reflection, such as seen in Figure 10b, can arise from preferred (001) growth (e.g., the vertically aligned hexagon modification with the *c*-axis perpendicular to the substrate) or from a larger number of (001) faces (the common hexagonal rod morphology but with the *c*-axis parallel to the substrate). Although the SEM image of the films deposited from **3** are of low-resolution (Figure 10a), they appear to show clusters of vertically aligned plates which combine into pseudospherical aggregates; they are certainly not consistent with the more common hexagonal rod morphology.

Clearly, in the gas phase any weak intermolecular Zn···F interactions (such as in **5** or **7**) will have little, if any, influence on the film deposited, and the lack of halogen in the final film suggests that decomposition eliminates the fluorocarbon groups, as, for example, $(R_f)_2CO$ or $[(R_f)_2CO]_2O$ by analogy with the decomposition of $Zn(O_2CCH_3)_2$.[39]

TGA data for the TMEDA adducts $RZnO_2CR_f$·TMEDA (**9**−**12**) (Figure 11) show relatively consistent behavior with no distinction between compounds with different $R_f$ groups. Data for **11** show a three stage process, starting with loss of the ethyl group (observed residual mass 87.4, theoretical 92.2%), then loss of TMEDA (observed residual mass 61.3, theoretical 61.0%), and finally decomposition of the carboxylate group

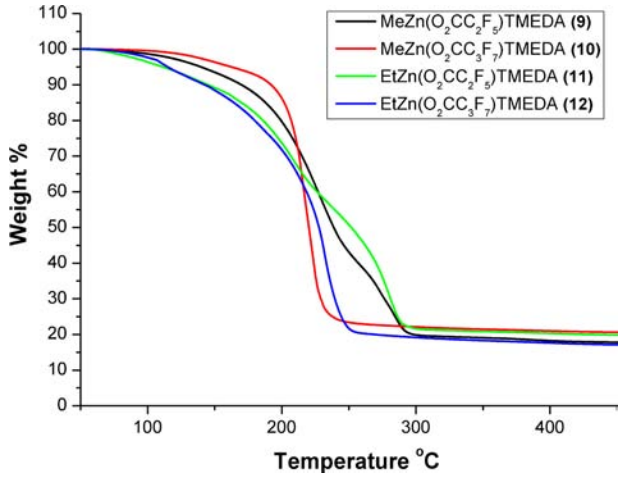


**Figure 11.** TGA data for $RZnO_2CR_f$·TMEDA (**9**−**12**).

leaving a residual mass of 21.4% compared to 21.5% expected for ZnO. It is likely that the remaining compounds **9**, **10**, **12** follow a similar pattern, though the above steps are not as clearly differentiated as for **11**. Films grown using **10** as precursor by LPCVD (39.6 Torr) on glass substrates at a reactor temperature of 400 °C, with a line and bubbler temperature of 90 °C over a duration of 90 min lead to granular (100−150 nm in diameter) ZnO films oriented in the (002) direction (Supporting Information), very similar to those deposited from **3** (Figure 10); EDX showed no evidence for fluorine incorporation into the film, nor were the films conducting.

The purely inorganic precursors $Zn(O_2CR_f)_2$·TMEDA (**13**, **14**) decompose in essentially a single concerted step (Figure 12), though a second stage in the decomposition of **14** at $T >$

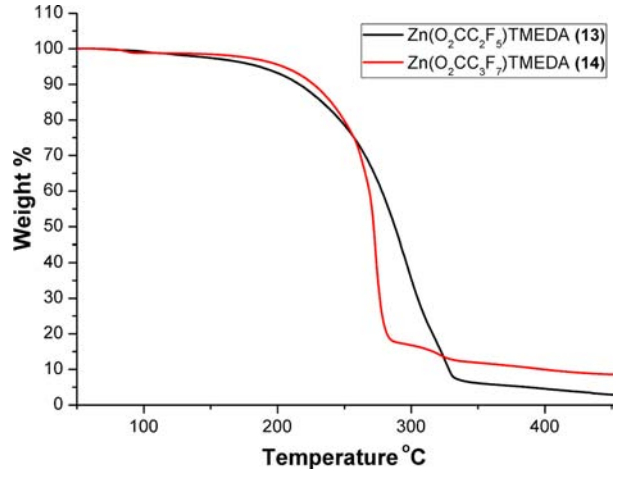


**Figure 12.** TGA data for $Zn(O_2CR_f)_2$·TMEDA (**13**, **14**).

290 °C is visible. In both cases the remaining residue at 350 °C (6.25, 12.3% for **13**, **14**, respectively) is less than that expected for ZnO (15.8, 13.2%, for **13**, **14**, respectively), indicating some volatility to these species.

LPCVD using **13** as precursor (glass substrate, reactor temperature 450 °C, bubbler and line temperatures 150 °C, 120 min, 39.8 Torr) yielded a textured, fluorine-free ZnO film comprising very small spheres (ca. 20 nm in diameter), cracked around clusters of varying size of these spheres. PXRD confirms


dx.doi.org/10.1021/ic400420h | *Inorg. Chem.* 2013, 52, 5515−5526

the films are ZnO but lack the preferred orientation shown in the films grown from **3** or **10** (Figure 13).

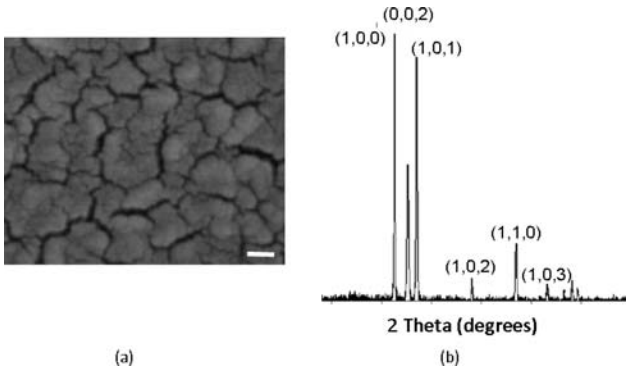


**Figure 13.** (a) SEM of the film grown from **13** by LPCVD, (b) PXRD of the film; indexing is to ZnO (PDF 89-1397).

## CONCLUSIONS

Zinc fluorocarboxylates, either $RZnO_2CR_f$, $RZnO_2CR_f$·TMEDA, or $Zn(O_2CR_f)_2$·TMEDA, can be used to deposit ZnO by LPCVD at 400 °C but do not result in measurable fluorine incorporation into the films. Conversely, $RZnO_2C_2F_5$, which shows close intermolecular Zn···F contacts in the solid state, decomposes in the bulk to $ZnF_2$. The only other report we can find concerning the synthesis of a single-source precursor for the deposition of ZnO:F relates to $EtZn[OC(Me)(CF_3)_2]$, but no materials chemistry was reported.[40] However, similar tin $[Sn(OCH(CF_3)_2)_4(HNMe_2)_2]$[41] and indium alkoxides $[In(OCMe(CF_3)_2)_3(H_2NBu^t)]$[42] do deposit fluorine-doped $SnO_2$ or $In_2O_3$, respectively. Interestingly, the incorporation of fluorine into $In_2O_3$ from the fluoroalkoxide does not occur at 550 °C, in contrast to 2−3 atom % at $T$ < 500 °C,[42] and in the case of ZnO:F (prepared by spray pyrolysis) the composition changes from $ZnO_{0.90}F_{0.10}$ at 400 °C to $ZnO_{0.94}F_{0.06}$ at 525 °C, that is, loss of dopant is relatively facile and thus temperature sensitive.[43] Moreover, in the structure of $[In(OCH(CF_3)_2)_4(H_2NBu^t)]^-[H_3NBu^t]^+$ there is a close intramolecular In···F contact (2.924 Å),[44] well within the sum of the van der Waals radii (3.45 Å) despite the fact that it incorporates five-coordinate indium. An even shorter In···F contact is present in $[In(OCMe(CF_3)_2)_3]_2$ (2.809 Å) which contains a four-coordinate metal,[44] and these, along with their intramolecular nature, may account for the success in the indium system which is lacking with our zinc compounds.

## ASSOCIATED CONTENT

### Supporting Information

Crystallographic data in CIF format. This material is available free of charge via the Internet at http://pubs.acs.org. Also, crystallographic data for the structural analysis (in CIF format) have been deposited with the Cambridge Crystallographic Data Center, CCDC nos. 910799−910806 for **2**, **5**−**8**, **11**, **13**, **15**, respectively. Copies of this information may be obtained from the Director, CCDC, 12 Union Road, Cambridge, CB21EZ, U.K. (Fax: +44-1233-336033; e-mail: deposit@ccdc.cam.ac.uk or www.ccdc.cam.ac.uk).

## AUTHOR INFORMATION

### Corresponding Author

*E-mail: chskcm@bath.ac.uk.

### Notes

The authors declare no competing financial interest.

## ACKNOWLEDGMENTS

We thank the EPSRC for funding (to A.L.S.) via the Supergen consortium.

## REFERENCES

(1) Lipscombe, W. N.; Strater, N. *Chem. Rev.* **1996**, *96*, 2375.
(2) Coates, G. W.; Moore, D. R. *Angew. Chem., Int. Ed.* **2004**, *43*, 6618.
(3) Orchard, K. L.; Harris, J. E.; White, A. J. P.; Shaffer, M. S. P.; Williams, C. K. *Organometallics* **2011**, *30*, 2223.
(4) Lorenz, J. C.; Long, J.; Yang, Z.; Xue, S.; Xie, Y.; Shi, Y. *J. Org. Chem.* **2004**, *69*, 327.
(5) Kuran, W. *Principles of Coordination Polymerization*; Wiley: Chichester, U.K., 2001.
(6) Redshaw, C.; Jana, S.; Shang, C.; Elsegood, M. R. J.; Lu, X.; Guo, Z. X. *Organometallics* **2010**, *29*, 6129.
(7) Tranchemontagn, D. J.; Mendoza-Cortés, J. L.; O'Keeffe, M.; Yaghi, O. M. *Chem. Soc. Rev.* **2009**, *38*, 1257.
(8) Bury, W.; Justyniak, I.; Prochowicz, D.; Rola-Noworyta, A.; Lewiński, J. *Inorg. Chem.* **2012**, *51*, 7410.
(9) Bury, W.; Justyniak, I.; Prochowicz, D.; Wróbel, Z.; Lewiński, J. *Chem. Commun.* **2012**, *48*, 7362.
(10) Liang, H. F.; Gordon, R. G. *J. Mater. Sci.* **2007**, *42*, 6388.
(11) Hu, J.; Gordon, R. G. *J. Electrochem. Soc.* **1992**, *139*, 2014.
(12) Hu, J.; Gordon, R. G. *J. Appl. Phys.* **1992**, *71*, 880.
(13) Hirata, G. A.; Siqueiros, J. M.; Diaz, J. A.; Contreras, O.; McKittrick, J.; Cheeks, T.; Lopez, O. A. *Thin Solid Films* **1996**, *288*, 29.
(14) de la L. Olvera, M.; Maldonado, A.; Asomoza, R.; Konagai, M.; Asomoza, M. *Thin Solid Films* **1993**, *229*, 196.
(15) Hu, J. H.; Gordon, R. G. *Sol. Cells* **1991**, *30*, 437.
(16) Gordon, R. G. *MRS Bull.* **2000**, *25*, 52.
(17) de la L. Olvera, M.; Maldonado, A.; Asomoza, R.; Solorza, O.; Acosta, D. R. *Thin Solid Films* **2001**, *394*, 241.
(18) Nam, G. M.; Kwon, M. S. *Electron. Mater. Lett.* **2011**, *7*, 127.
(19) Yoon, H. S.; Lee, K. S.; Lee, T. S.; Cheong, B.; Choi, D. K.; Kim, D. H.; Kim, W. M. *Sol. Energy Mater. Sol. Cells* **2008**, *92*, 1366.
(20) Mahon, M. F.; Molloy, K. C.; Stanley, J. E.; Rankin, D. W. H.; Robertson, H. E.; Johnston, B. F. *Appl. Organomet. Chem.* **2005**, *19*, 658.
(21) Karipides, A. *Acta Crystallogr., Sect.B: Struct. Crystallogr. Cryst. Chem.* **1980**, *36*, 1659.
(22) Ibrahim, K.; Sahin, O.; Filiz, Y.; Buyukgungor, O. *Acta Crystallogr., Sect. E: Struct. Rep. Online* **2006**, *62*, m1909.
(23) Farrugia, L. J. *J. Appl. Crystallogr.* **1999**, *32*, 837.
(24) Lewiński, J.; Bury, W.; Dutkiewicz; Maurin, M.; Justyniak, I.; Lipkowski, J. *Angew. Chem., Int. Ed. Engl.* **2008**, *47*, 573.
(25) Lewiński, J.; Marciniak, W.; Lipkowski, J.; Justyniak, I. *J. Am. Chem. Soc.* **2003**, *125*, 12698.
(26) Hollingsworth, N.; Johnson, A. L.; Kingsley, A.; Kociok-Köhn, G.; Molloy, K. C. *Organometallics* **2010**, *29*, 3318.
(27) Lewiński, J.; Suwala, K.; Kubisiak, M.; Ochal, Z.; Justyniak, I.; Lipkowski, J. *Angew. Chem., Int. Ed.* **2008**, *47*, 7888.
(28) Dickie, D. A.; Jennings, M. C.; Jenkins, H. A.; Clyburne, J. A. C. *Inorg. Chem.* **2005**, *44*, 828.
(29) Lalioti, N.; Perlepes, S. P.; Manessi-Zoupa, E.; Raptopoulou, C. P.; Terzis, A.; Aliev, A. E.; Gerothanassis, I. P. *Chem. Commun.* **1998**, 1513.
(30) Addison, A. W.; Rao, T. N.; Reedijk, J.; van Rijn, J.; Verschoor, G. C. *J. Chem. Soc., Dalton Trans.* **1984**, 1349.
(31) Orchard, K. L.; White, A. J. P.; Shaffer, M. S. P.; Williams, C. K. *Organometallics* **2009**, *28*, 5828.

(32) Orchard, K. L.; Harris, J. E.; White, A. J. P.; Shaffer, M. S. P.; Williams, C. K. *Organometallics* **2011**, *30*, 2223.
(33) Brown, D. A.; Errington, W.; Fitzpatrick, N. J.; Glass, W. K.; Kemp, T. J.; Nimir, H.; Ryan, A. T. *Chem. Commun.* **2002**, 1210.
(34) Brown, D. A.; Fitzpatrick, N. J.; Muller-Bunz, H.; Ryan, A. T. *Inorg. Chem.* **2006**, *45*, 4497.
(35) Lingg, L. J.; Berry, A. D.; Purdy, A. P.; Ewing, K. J. *Thin Solid Films* **1992**, *209*, 9.
(36) Liu, X.; Afzaal, M.; Ramasamy, K.; O'Brien, P.; Akhtar, J. *J. Am. Chem. Soc.* **2009**, *131*, 15106.
(37) Liu, X.; Afzaal, M.; Badcock, T.; Dawson, P.; O'Brien, P. *Mater. Chem. Phys.* **2011**, *127*, 174.
(38) Barreca, D.; Ferrucci, A. P.; Gasparotto, A.; Maccato, C.; Maragno, C.; Tondello, E. *Chem. Vap. Deposition* **2007**, *13*, 618.
(39) Duan, Y.; Li, J.; Yang, X.; Hu, L.; Wang, Z.; Liu, Y.; Wang, C. *J. Anal. Appl. Pyrol.* **2008**, *83*, 1.
(40) Suh, S.; Mîinea, L. A.; Javed, S.; Hoffman, D. M. *Polyhedron* **2008**, *27*, 513.
(41) Suh, S.; Hoffman, D. M.; Atagi, L. M.; Smith, D. C.; Liu, J.-R.; Chu, W.-K. *Chem. Mater.* **1997**, *9*, 730.
(42) Mîinea, L. A.; Hoffman, D. M. *J. Mater. Chem.* **2000**, *10*, 2392.
(43) Castañeda, L.; Maldonado, A.; Cheang-Wong, J. C.; Terronese, M.; de la L. Olvera, M. *Phys. B* **2007**, *390*, 10.
(44) Mîinea, L. A.; Suh, S.; Hoffman, D. M. *Inorg. Chem.* **1999**, *38*, 4444.